SEGMENTATION AND CHARACTERIZATION OF SURFACE FEATURES TO AID COMPUTATIONAL MODELLING OF NICKEL SUPERALLOY 625 AS-BUILT LASER POWDER BED FUSION PARTS

Jason C. Fox[1] and Chris J. Evans[1,2]
[1]Intelligent Systems Division
National Institute of Standards and Technology
Gaithersburg, MD, USA
[2]Center for Precision Metrology
University of North Carolina at Charlotte
Charlotte, NC, USA

The lack of strong correlations between the as-built surface topography of AM parts and heat-transfer efficiency inhibits development for these applications. This issue stems from the complex and multi-scale surface topography along with significant variability in builds when compared to traditional fabrication methods. Correlation development can benefit from computational thermal and fluid modelling; but the large range of relevant scales on as-built surfaces make computation times impractical. To address this, data from a publicly available dataset of nickel superalloy 625 surfaces built in a laser powder bed fusion system are analyzed. Advanced characterization techniques and a segmentation technique developed by the authors are used to identify key features relevant to heat transfer. Analysis of the areal parameter Str shows correlation to the particle content of a surface. Particle segmentation creates attenuation of amplitude wavelength plots, particularly at the short wavelengths. Gaussian filters can be used to remove discontinuities and particles can be added arithmetically back to the surface based on segmentation data. Further simplifications of the surfaces are also presented. These methods provide simplifications that will reduce computational load and a foundation for experimental and modelling studies to come.

INTRODUCTION

Additive manufacturing (AM) and laser powder bed fusion (LPBF) show tremendous potential in heat transfer applications due to the ability to create complex channels, not achievable through traditional manufacturing [1]. Additionally, the as-built surface finish can be beneficial to heat transfer by increasing surface area [2,3] in some cases. As-built AM surfaces, however, are complex and cover a wide range of size scales, challenging our ability to develop relevant correlations between surface texture parameters and performance in heat-transfer applications [4].

The concept of using AM components for heat transfer applications is not novel and has been studied in other works. Neugebauer et al. investigated the effect of surface roughness on heat exchanger performance and found that the AM component provided improved properties over the conventionally manufactured component [2]. Kirsch and Thole found that channels with short wavelength-dominant surface designs resulted in high pressure losses without a corresponding increase in heat transfer [3]. Alshare et al. were able to improve performance of a hydraulic manifold by manufacturing with AM and optimizing the design a priori using computational fluid dynamics (CFD) simulations [5]. Mandloi et al. found that the “lay” of the surface based on melt tracks or staircasing effects relative to fluid flow and position of particles on the surface can influence the heat transfer efficiency [6].

Zhang et al. recently reviewed literature on AM fabricated fluid channels and found that a key barrier is controlling the forming qualities (i.e., surface finish and contour accuracy) of internal channels [1]. While there is difficulty in controlling the forming qualities, the authors argue more detailed metrology will provide insights to the nature of the variabilities. Many groups have investigated these techniques and, although not always for heat transfer applications, have had success in better understanding the complex topographies that make up the as-built AM surface.

Senin et al. developed techniques for feature-based characterization of AM top surfaces by segmenting particles, weld tracks, and weld

ripples [7]. Default build parameters in commercial AM machines can result in local variation in weld track width and amplitude [8] and meso scale melt pool distortions [9]. Reese et al. investigated the relationship between melt pool geometry and chevron patterns on single-track experiments [10]. Newton et al. investigated and compared segmentation methods for isolating powder particles on the surface of AM parts [11].

Even with an ever-improving understanding of topographies found on AM surfaces, a difficulty remains in understanding the relationship these surfaces have to performance in heat transfer applications. While modelling can aid this understanding, the multi-scale nature of AM surfaces can make modelling as-built AM surfaces computationally prohibitive [4].

To address these issues, the authors analyze surface topographies from a publicly available data set of 648 as-built LPBF nickel superalloy 625 (IN625) surfaces from a single build on an EOS M290 system [12]. Methods developed in Fox et al. [4] are applied to surfaces with a wide range of build positions and orientations to determine if previous analyses hold across the build volume. Areal parameters, segmented particles and surfaces, and amplitude-wavelength (AW) data are analyzed to assess the capability of the segmentation method. This data is also used to identify surface simplifications and substitute geometries that approximate real AM surfaces and particles while lessening the computational burden of thermal and fluid simulations in preparation for comparison of modelling and experimental efforts [6].

METHODS

Experiment Data, Parameter Calculation, and Segmentation

Full details of the build, sample preparation, and measurement are available in Fox, 2019 [12]. For brevity, the same naming conventions for sample, rib, and surface numbers will be used. Most relevant to this work is that Surf1 to Surf9 were built at angles of 165° to 45°, respectively, as measured from the build plate and in 15° increments. STV1 through STV9 identify the different artifacts in the build. Rib1 through Rib8 identify the eight sets of surfaces (i.e., Surf1 to Surf 9) on the artifact. Areal surface parameters were calculated using the publicly available OmniSurf3D software.

For segmentation, particles were identified using a filter, threshold, and mask methodology developed by the authors [4]. In this method, the surfaces are filtered with digital Gaussian filters (S-filter = 2.5 µm and L-filter = 80 µm). The S-filter was chosen as five times the point spacing per ASME B46.1 and ISO 25718-3 [13,14]. The L-filter was chosen to accentuate the particles attached to the surface, as reclaimed powder in this build is passed through an 80 µm sieve. The areal parameter for the Core Height (Sk) is calculated on the filtered surfaces, then thresholded at Sk/2 above the mean plane. In theory, this should just include the peaks (i.e., particles) and the melt surface should remain below half the core height above the mean plane. A mask is then created to identify any points above the threshold as particles. This mask is then applied to a surface filtered with S-filter = 2.5 µm and L-filter = 2.5 mm. This L-filter was chosen as it is the largest standard filter that fits within the width of the surface (4 mm). In situations where the desired outcome is to fully remove the particle from the surface, the mask is dilated by 10 points (5 µm). In situations where sizes or heights of the particles are calculated, the mask is not dilated. In either case it is stated explicitly.

Amplitude-Wavelength Analysis

Fourier analysis is commonly used to evaluate contributions to a surface at different spatial frequencies or wavelengths, often using the Power Spectrum Density (PSD). Area PSDs are sometimes used to specify or visualize surfaces of high-quality optics. This visualization is not intuitive (He et al. [15]), even to many optical engineers. It presupposes that low order waviness is removed before calculation, invoking what is known in optics as “Church’s rule” (named for pioneer in optical scattering from “smooth” surfaces E. Church) that the 3 lowest frequencies are suspect and should be ignored. In AW plots, the visualization provides half the peak to valley distance at any wavelength and, therefore, a more intuitive sense of which wavelengths are dominant. For these reasons, AW analysis is used.

The AM surfaces considered in this work have a strong lay, arising from the locally uni-directional laser spot trajectory (for “top” surfaces) and/or the staircase effect for surfaces not parallel to the build plane; the “rise” in the staircase is always the nominal layer thickness (40 µm in this work), while the “run” depends on the angle of the

surface (see Table 1 in [4]). While there is variation along the lay, it is minor compared to across the lay. In this work, we constrain our consideration to heat transfer arising from flow across the lay in a nominal cooling channel. Hence, the averaged PSD of columns of height data orthogonal to the lay may describe the topographical contribution (with appropriate caveats) to heat transfer and fluid flow in a cooling channel.

All AW analyses presented here for measured surfaces use the amplitude (half the peak-to-valley distance) vs wavelength with smoothing set at 25 (see FIGURE 1), as do all evaluations of segmented surface features unless otherwise stated. The latter statement introduces some questions. Consider, for example, our discussion of substitute geometries ("Simplified Melt Surfaces and Particles" section). We apply a low pass filter (chosen between 8 µm and 11 µm, not to be harmonic with the evaluation length) to eliminate discontinuities. For example, the AW plot for Surface 1 sawtooth with 8 µm robust Gaussian filter, FIGURE 8, shows a main peak at 155 microns, with tails (≈ 2.5 % of peak) at 120 µm and 200 µm. There is also a broad, flat-topped, low amplitude, first harmonic (758 µm). Eliminating the filter has no effect on the peak wavelength (to sub-µm resolution), and 5 % effect in peak amplitude. The effect of the filter increases as the wavelength decreases.

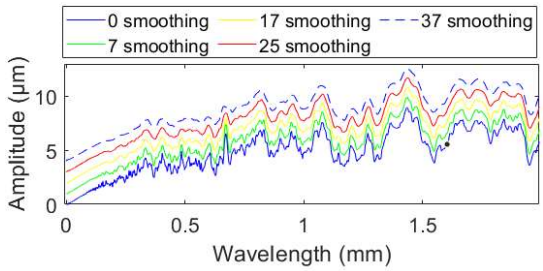

FIGURE 1. AW profiles as a function of "smoothing" offset by 1 mm from 0 to 37.

RESULTS

The areal parameter surface texture aspect ratio (Str), which is a measure of the spatial isotropy, is hypothesized to differentiate between surfaces dominated by powder particles and surfaces dominated by the melt surface [4]. With this parameter, the former will exhibit a very isotropic surface (i.e., Str close to 1) and the latter will exhibit a dominant lay (i.e., Str close to zero). The Str values of the 648 surfaces exhibit the hypothesized differentiation (see FIGURE 2).

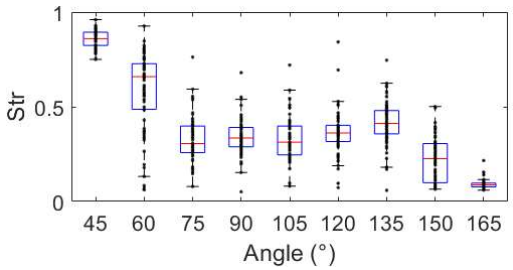

FIGURE 2. Str for data from Fox 2019 [12]. *Digital Gaussian S-filter = 2.5 µm and L-filter = 2.5 mm. Levelled using a mean plane with vertical residuals. No fill was applied to the data.*

Re-calculation of Str after particle removal with dilation described in the "Methods" section shows a dramatic decrease in Str values (FIGURE 3). This was only performed on surfaces of 75 ° to 165° as the 60° and 45° surfaces are particle dominated and do not provide sufficient melt surface for parameter calculation after removal. In the case of the 165° surfaces, a slight increase in Str is attributed to the tops of undulations in the melt surface being captured by the threshold masking. Adjustment of the filters and threshold value, however, should prevent this issue [4].

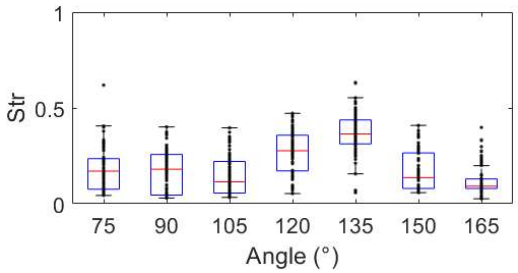

FIGURE 3. Str for data from Fox 2019 [12] *after removal of particles. Digital Gaussian S-filter = 2.5 µm and L-filter = 2.5 mm. Levelled using a mean plane with vertical residuals. No fill was applied to the data.*

With particles segmented, analysis of the particles and melt surface separately can aid in understanding methods to simplify surfaces for modelling studies. Equivalent diameter, which is defined here as the diameter of a circle with equivalent footprint area to a segmented particle, and position can be determined from the segmentation. An example of this for a single surface is shown in FIGURE 4. This, along with many other statistics can be captured and analyzed to make intelligent alterations to surface geometries. The equivalent diameter can be used to make estimations of the size of particles attached. This information can then be used to simplify surfaces by improving mesh

characteristics or even altering geometry of the particles to reduce computational load with minimal effect on simulation results [16].

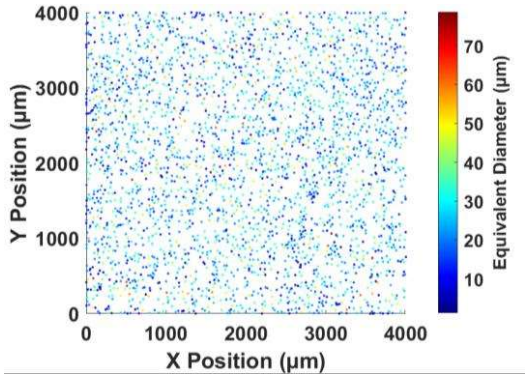

FIGURE 4. Equivalent diameter by position on STV1 Rib2 Surf5.

The hypothesis from prior work that the mean height of particles on the surface transitioned from above the mean plane to below the mean plane for upward facing versus downward facing surfaces [4]. This relationship held across all the surfaces analyzed.

Amplitude Wavelength

AW analyses of surfaces before particle removal did not exhibit clear and consistent dominant peaks that correlated to the build process. After segmentation of particles with dilation, a distinct decrease in the amplitude of short wavelengths of the AW data can be seen in FIGURE 5. The decrease in amplitude is seen in wavelengths up to ≈ 400 µm, after which, most peaks remain, though slightly attenuated. This suggests that the particle contribution to the surface will be concentrated in the shorter wavelengths and longer wavelengths will provide details on the melt surface, as expected. This is also consistent with Kirsch and Thole [3] and Mandloi et al. [6]. Kirsch and Thole found that shorter wavelengths on the surface create pressure losses without increasing heat transfer [3]. Mandloi et al found that particles create stagnation points that inhibit both the flow and heat transfer [6].

Additionally, AW data for the original surface measurement (≈ 1.5 % Non-Measured (NM) points), after removing particles (≈ 30 % NM) and filling the NM points in Mountains is shown. Particle-removed and Mountains-NM-filled surfaces are shown in FIGURE 6 and FIGURE 7. The Mountains NM fill tracks well to the particles removed, suggesting that this approach reasonably allows us to remove discontinuities in the raw data that we process to use in CFD simulations (meshing permitting).

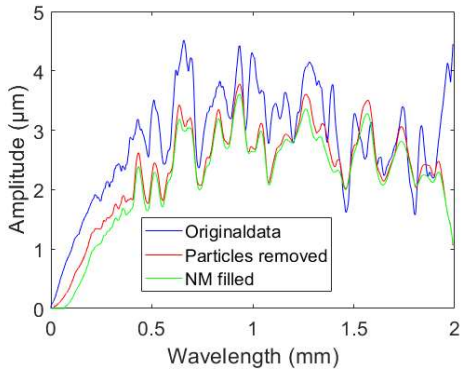

FIGURE 5. AW analysis of STV1 Rib2 Surf5. Original (blue), particle removed (red), and data using Mountains to fill NM points (green).

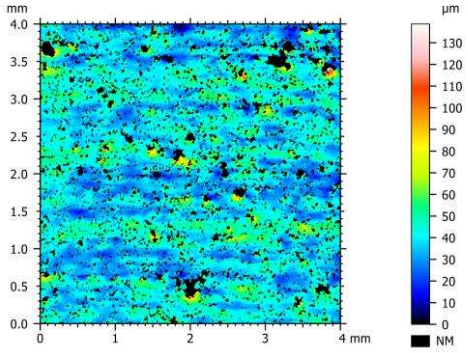

FIGURE 6. STV1 Rib2 Surf5 particle removed with ten-pixel dilation.

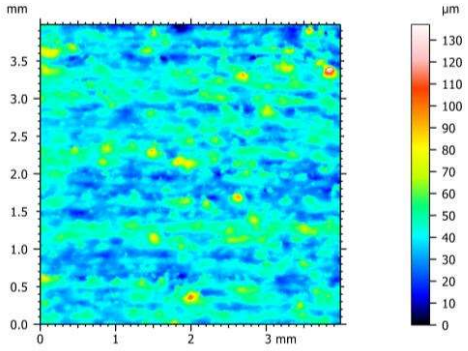

FIGURE 7. The surface from FIGURE 6 after Mountains NM fill and 8 µm robust Gaussian low-pass filter.

Comparison of AW results show that there is little change to the longer wavelength portion of the spectrum, suggesting that this method can be used to greatly simplify a surface. Additionally, we can use the information from the particle segmentation to add the particles back to the

surface arithmetically. This can be performed using the equivalent diameter and position data (e.g., data from FIGURE 4). This, in theory, should allow for the removal of large discontinuities without affecting the key spatial wavelengths that are relevant to fluid flow and heat transfer.

Simplified Melt Surfaces and Particles

While analysis of mesh size and surface complexity is forthcoming, these surfaces may still be too computationally expensive to use in thermal-fluid models. In response to this, the authors have taken a second approach, moving from overly simplified toward more realistic. In this case, the authors have simulated surfaces based on the staircasing effect. In LPBF AM, the staircasing effect occurs because the parts are built as multiple areas with finite thickness stacked on top of each other [17]. As such, the stepover can be approximated based on the angle of the surface and the layer thickness (see table 1 in Fox et al. [4]). With this approach, the authors created two simulated surfaces that have the proper stepover and layer thickness for the given angle. AW of these surfaces, shown in FIGURE 8, have broad peaks at the expected staircase distance and the associated harmonics. Furthermore, particles can be added to the surface based on the position and size characteristics, (e.g., the data in FIGURE 4 for STV1 Rib2 Surf5). The particles can also be investigated for simplifications by creating rectangular, cylindrical, or pyramidal shaped particles instead of spherical, which require many elements to replicate the shape. The simplified particles can be created with matching surface area or volume to segmented particle data. While these possibilities are highly simplified, they can be tested along with the other surfaces to determine if the simplified surfaces and particles still provide reasonable results while benefiting from the reduced computational load [16].

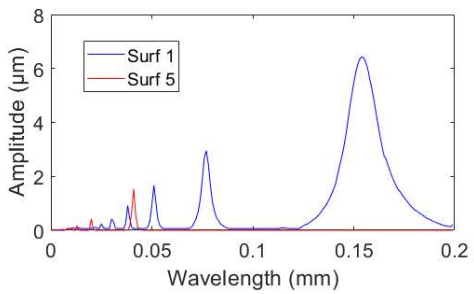

FIGURE 8. AW analysis of two sawtooth surfaces.

Conclusions and Future Work

Surface-height data was analyzed with advanced surface characterization techniques and several methods to simplify surfaces and reduce computational load in thermal and fluid dynamics simulations were presented. Data used in this study was from a publicly available dataset of IN625 samples built by LPBF on an EOS M290 system [12]. Segmentation of particles was performed on all surfaces using a novel filter, threshold, mask methodology developed by the authors [4]. The relationship between surface angle and mean height of particles shifting from above the mean plane on upward facing surfaces to below the mean plane on downward facing ones previously seen in Fox et al. [4] was found across all samples. Analysis of the areal parameter Str also showed correlation to the amount of attached powder particles on the surface. This correlation held across all 648 samples in the dataset and Str decreased dramatically when particles were removed from the surface via segmentation.

AW analysis of surfaces before and after particle segmentation show a clear decrease in amplitude up to ≈ 400 µm, after which peaks remain though slightly attenuated. Filling the NM points using the Mountains software and filtering with an 8 µm digital Gaussian filter showed little difference to the particle removed surfaces. These results suggest that the longer wavelength contributions can be preserved while discontinuities are removed. Filling algorithms also pose potential for extrapolation errors, which must also be investigated. It is also hypothesized that the short wavelength content can be preserved through adding the particles back to the surface based on data captured during segmentation.

Highly simplified surfaces based on the staircasing effect were also presented. While these surfaces may not be realistic compared to the height data, they maintain an important characteristic of the surface while allowing for decreased computational load in modelling studies. Current ongoing and future work include quantitative assessment of how all the surface simplifications presented can decrease modelling time in thermal-fluid simulations. These model results will also be compared to experiments using the setup described in Mandloi et al. [6] to determine their accuracy as well.

ACKNOWLEDGEMENTS

The authors would like to thank H. Cherukuri and K. Mandloi for their input on the modelling directions. The authors would also like to thank the UNCC Center for precision metrology and NIST for the support of this work.

DISCLAIMER

Certain commercial entities, equipment, or materials may be identified in this document to describe an experimental procedure or concept adequately. Such identification is not intended to imply recommendation or endorsement by the National Institute of Standards and Technology, nor is it intended to imply that the entities, materials, or equipment are necessarily the best available for the purpose. Contributions of NIST not subject to US Copyright.

REFERENCES

[1] C. Zhang, S. Wang, J. Li, Y. Zhu, T. Peng, H. Yang, Additive manufacturing of products with functional fluid channels: A review, Addit. Manuf. 36 (2020) 101490.

[2] R. Neugebauer, B. Müller, M. Gebauer, T. Töppel, Additive manufacturing boosts efficiency of heat transfer components, Assem. Autom. 31 (2011) 344–347.

[3] K.L. Kirsch, K.A. Thole, Heat Transfer and Pressure Loss Measurements in Additively Manufactured Wavy Microchannels, J. Turbomach. 139 (2016).

[4] J.C. Fox, C. Evans, K. Mandloi, Characterization of LPBF surfaces for heat transfer applications, CIRP Ann. 70 (2021) 467–470.

[5] A.A. Alshare, F. Calzone, M. Muzzupappa, Hydraulic manifold design via additive manufacturing optimized with CFD and fluid-structure interaction simulations, Rapid Prototyp. J. 25 (2019) 1516–1524.

[6] K. Mandloi, C. Evans, J. Fox, H. Cherukuri, J. Miller, A. Allen, D. Deisenroth, M. Donmez, Toward specification of complex additive manufactured metal surfaces for optimum heat transfer., in: Proc. Jt. Spec. Interest Group Meet. Euspen ASPE, St. Gallen, Switzerland, 2021.

[7] N. Senin, A. Thompson, R. Leach, Feature-based characterisation of signature topography in laser powder bed fusion of metals, Meas. Sci. Technol. 29 (2018) 045009.

[8] J.C. Fox, A. Sood, R. Isaacs, P. Brackman, B. Mullany, E. Morse, A. Allen, E.C. Santos, C. Evans, Surface Feature Characteristics of LPBF of Nickel Super Alloy 625 Bulk Regions, Procedia CIRP. 108 (2022) 531–536.

[9] J.C. Fox, C. Evans, A. Sood, R. Isaacs, B. Mullany, A.D. Allen, E. Morse, Weld Track Distortion In Laser Powder Bed Fusion Of Nickel Superalloy 625, in: Proc. ASPE-Euspen SIG Meet. Adv. Precis. AM, Oak Ridge, TN, 2022.

[10] Z.C. Reese, J.C. Fox, J. Taylor, C. Evans, Evolution of Cooling Length in Parts Created Through Laser Powder Bed Fusion Additive Manufacturing, in: Proc. 2018 ASPE Euspen Summer Top. Meet. - Adv. Precis. Addit. Manuf., Berkeley, CA, 2018: pp. 183–188.

[11] L. Newton, N. Senin, B. Smith, E. Chatzivagiannis, R. Leach, Comparison and validation of surface topography segmentation methods for feature-based characterisation of metal powder bed fusion surfaces, Surf. Topogr. Metrol. Prop. 7 (2019) 045020.

[12] J.C. Fox, Variation of Surface Topography in Laser Powder Bed Fusion Additive Manufacturing of Nickel Super Alloy 625, J. Res. Natl. Inst. Stand. Technol. 124 (2019).

[13] ASME B46.1: Surface Texture (Surface Roughness, Waviness, and Lay), New York, NY, (2019).

[14] ISO 25178-3:2012 - Geometrical Product Specifications (GPS) - Surface Texture: Areal - Part 3: Specification operators, ISO, Geneva., (2012).

[15] L. He, C.J. Evans, A. Davies, Optical surface characterization with the area structure function, CIRP Ann. 62 (2013) 539–542.

[16] K. Mandloi, C. Evans, J.C. Fox, H. Cherukuri, J. Miller, A. Allen, J. Raquet, B. Dutterer, The Impact of Additive Manufacturing Surface Characteristics for Heat Transfer Applications, in: Proc. ASPE-Euspen SIG Meet. Adv. Precis. AM, Oak Ridge, TN, 2022.

[17] F. Cabanettes, A. Joubert, G. Chardon, V. Dumas, J. Rech, C. Grosjean, Z. Dimkovski, Topography of as built surfaces generated in metal additive manufacturing: A multi scale analysis from form to roughness, Precis. Eng. 52 (2018) 249–265.